



Experimental and theoretical investigation on the correlation between aqueous precursors structure and crystalline phases of zirconia

Shou-Gang Chen^{a,*}, Yan-Sheng Yin^a, Dao-Ping Wang^b

^aKey Lab of Liquid Structure and Heredity of Materials, Ministry of Education, Key Lab of Engineering Ceramic of Shandong Province, School of Materials, Shandong University, Jinan 250061, China

^bSchool of Chemistry, Chemical Engineering and Materials Science, Shandong Normal University, Jinan 250014, China

Received 11 July 2003; revised 3 December 2003; accepted 4 December 2003

Abstract

Nanometer zirconia powders were prepared by the precipitation method at different pHs and different reaction temperatures. X-ray results show that monoclinic zirconia is favored at pH 4 while tetragonal zirconia is favored at pH 9.5 at room temperature, and monoclinic zirconia is also favored at pH 9.5 and 70 °C reaction temperature, with the slow addition of alkali. Four models of zirconium complexes were applied to simulate the structural monomers in different pH solutions. Geometric parameters and Mulliken charge population were calculated by optimizing these complexes using the density functional theory (DFT/B3LYP). Theoretical analyses show that if Model I ($[\text{Zr}(\text{OH})_2(\text{H}_2\text{O})_4]^{2+}$ monomers) is favored in the aqueous precursor solution, it will be preferentially polymerized into monoclinic precursor structure irrespective of slow or quick alkali addition. Contrarily, if Model IV ($[\text{Zr}(\text{OH})_7]^{3-}$ monomers) is major in the aqueous precursor solution, tetragonal precursor structures are favored irrespective of slow or quick alkali addition. When Model II ($[\text{Zr}(\text{OH})_4(\text{H}_2\text{O})_2]^0$ monomers) and Model III ($[\text{Zr}(\text{OH})_6]^{2-}$ monomers), respectively, predominate in the aqueous precursor solution, they will be preferentially polymerized into tetragonal precursor structure at slow alkali addition, however, for quick alkali addition, they will be preferentially polymerized into monoclinic precursor structure. Our theoretical models well explain the present experimental results as well as previous experimental results, and allow building up a correlation between aqueous precursor structures and crystalline phases of zirconia.

© 2004 Elsevier B.V. All rights reserved.

Keywords: Zirconia; Precipitation; X-ray diffraction; Density functional theory/B3LYP; Mulliken charge population

1. Introduction

Zirconia-based ceramics have gained great attention as engineering ceramics and catalysis materials because of their diverse commercial applications. Research on the metastable phases of these materials and their transitions have been a subject of great scientific and technological importance during recent years. A number of explanations have been offered for the interpretation of the presence of metastable tetragonal as well as cubic zirconia structures at low temperature. Garvie attributed it to crystallite size effects [1], Wu and Yu [2] attributed it to strain and lattice defects, Clearfield [3] attributed it to the rate of polymerization of the Zr^{4+} species, Livage [4] attributed it to the short-range structural similarities

of the amorphous precursor and the tetragonal phase, and other authors attributed it to the existence of a certain number of oxygen vacancies [5].

Precipitation and sol–gel methods are the most used chemical methods to produce zirconia nanoparticles. The precipitation-driven product is indeed more hydrous, and consequently, its complex molecular structure contains various amounts of water in the form of hydrous oxide $\text{ZrO}_2 \cdot \text{H}_2\text{O}$ or $\text{ZrO}(\text{OH})_2$. Sol–gel chemistry is also based on inorganic polymerization reactions. This process involves the use of molecular precursors, mainly alkoxides as starting materials. Hence, the aqueous chemistry of zirconium is dominated by its tendency to form inorganic polymers based on bridged-hydroxyl groups whether using the precipitation method or the sol–gel method [6]. During polymeric progress, the monomers structures play a significant role in the final gel molecular precursor structure [7], and the different structural

* Corresponding author. Tel./fax: +86-531-8392439.

E-mail address: sgchen2000@yahoo.com.cn (S.-G. Chen).

monomers will produce different reaction processes [8]. Recently, Caracoche et al. [9] synthesized nanometer zirconia powders using the sol–gel method at different pHs. Their experimental results indicate that the different morphology and structure of precursor gels were determined by the extent of condensation, which is in turn affected by the pH value of the precursor solution. However, there exist some other arguments on the formation of amorphous precursor structure for the monoclinic and/or the tetragonal phases in different pH solutions [10–12]. In this investigation, we synthesize nanometer zirconia powders using a precipitation method at different pHs and different reaction temperatures. Interestingly, our experimental results show that monoclinic zirconia could be attained not only at a low pH but also at high pH and a higher reaction temperature. The detailed analysis shows that different precursor structures in the solution are very important for the crystal phases obtained. Thus, it is necessary to clarify the correlation between the precursor structures of the aqueous solution and the final crystalline phases of zirconia.

Computational quantum chemistry provides a detailed description of the bonding, charge distribution, structure preferences and geometry of molecular materials [7,13], especially the development of Density Functional Theory (DFT). Based on the idea that a theoretical study would help us to further understand the correlation between the precursor structure and the microstructure of prepared samples, our research group decided to explore the electronic structure of four zirconium complexes models related to different pH solutions, namely, (I) $[\text{Zr}(\text{OH})_2(\text{H}_2\text{O})_4]^{2+}$ ($\text{pH} < 7$); (II) $[\text{Zr}(\text{OH})_4(\text{H}_2\text{O})_2]^0$ ($\text{pH} \approx 7$); (III) $[\text{Zr}(\text{OH})_6]^{2-}$ ($7 < \text{pH} \leq 10.5$) and (IV) $[\text{Zr}(\text{OH})_7]^{3-}$ ($10.5 \leq \text{pH} \leq 14$).

2. Experimental procedures and computational method

2.1. Experimental procedures

Two samples of hydrous ZrO_2 were prepared using the precipitation method from a $\text{ZrOCl}_2 \cdot 8\text{H}_2\text{O}$ (Tianda, China, purity of 99%) solution (0.1 M) with 2 mass% polyglycol (PEG, molecular weight 20,000 g/mol) by the slow addition of the NH_4OH (25%) solution, respectively, needed to produce desired pHs of 4 and 9.5. The resulting precipitates were repeatedly centrifugally washed with deionized water at 8000 n/min until a negative test for Cl^- , and then centrifugally washed twice with anhydrous ethanol at 8000 n/min. Further, the obtained gels were dried at 100°C for 24 h. In addition, we also prepared another hydrous ZrO_2 sample at 70°C water bath by the slower addition of the NH_4OH (25%) solution needed to produce a desired pH of 9.5 using the same precursor solution. The washing and dried process was carried out as mentioned above. Subsequently, the different hydrous ZrO_2 powders

were calcined for 2 h at different temperatures (450 and 600°C).

Crystalline species in zirconia powders were identified using an X-ray diffraction (XRD: Model D/MAX-RB12X, Rigaku Co., Tokyo, Japan). The scans were taken within the range of 10 – 80° (2θ) using $\text{Cu K}\alpha$ radiation. The volume fraction of the monoclinic phase (V_m) was determined by the empirical formula [14]

$$V_m = [I_m(111) + I_m(11\bar{1})]/[I_m(111) + I_m(11\bar{1}) + I_t(111)]$$

where I_m denotes the intensity of the monoclinic peak and I_t denotes the intensity of the tetragonal peak. The mean crystallite size was calculated by means of the line-broadening method from the measurement of the full width at half-maximum (FWHM) of the peak corresponding to the (111) reflections of the tetragonal or cubic zirconia phase. The mean value of crystallite size was estimated using the following equation of Scherrer and Warren [15]:

$$D_t = 0.9\lambda/(B^2 - b^2)^{1/2} \cos \theta_B$$

where D_t is the mean crystallite size, λ (0.15418 nm) and θ_B , respectively, denote the wavelength of the X-ray and the Bragg diffraction angle, and B and b denote the FWHMs observed for the present sample and the standard sample, respectively.

Differential thermal analysis (DTA) was also carried out to study the transformation of hydrous ZrO_2 samples using a DTA-40M analyzer (Japan). Measurements were carried out in the temperature range of 30 – 830°C at a $20^\circ\text{C}/\text{min}$ heating rate.

2.2. Computational method

Computations were performed using the GAUSSIAN 98 series of programs in Ref. [16]. Specifically, we used the B3LYP gradient-corrected DFT program [17]. Zr atoms are described using the Los Alamos Lanl2 effective core potentials (ECP) and a valence double- ξ basis set [18] while O and H atoms are described using the 6-31G(d) basis set [19]. These geometries are fully optimized to find stationary points followed by frequency calculations.

3. Results and discussion

3.1. Experimental results

Table 1 shows the crystallite size and phase volume fraction of zirconia powders obtained from different pH solutions and different reaction temperatures. The XRD analysis of Fig. 1a was performed on ZrO_2 xerogel obtained from a pH 4 solution and thermally treated at 600°C , for which 90.91% volume fraction of monoclinic zirconia was determined. The XRD analysis performed on ZrO_2 xerogel obtained from a pH 9.5 solution and thermally treated at 600°C (Fig. 1b) led to only 35.48% volume fraction of

Table 1
Crystallite size and phase volume fraction at different temperatures and different pH values

pHs	Temperature (°C)		Crystallite size (nm)		Phase volume fraction	
	Reaction	Calcining	Tetragonal	Monoclinic	Tetragonal	Monoclinic
4	25	450	11.530	15.768	17.30	82.70
4	25	600	17.243	43.199	9.09	90.91
9.5	25	600	15.141	23.763	64.52	35.48
9.5	70	600	17.382	33.145	18.98	81.02

monoclinic phase. It is obvious that monoclinic zirconia is the preferential crystalline phase at the lower pH value and tetragonal zirconia is the preferential crystalline phase at the higher pH value, for the same rate of alkali addition. Using Scherrer's equation [15], the average crystallite size ($D_t = 17.243$ nm) of tetragonal zirconia was obtained from the data of Fig. 1a. Based on Garvie's viewpoint [1], this crystalline size has not reached the critical size (30 nm) for the tetragonal-to-monoclinic phase transformation, but it has attained it according to other researchers' viewpoints [20–22]. Thus, we did not exclude the possibility that the existing monoclinic zirconia could come from the tetragonal-to-monoclinic phase transformation. In order to

explore the real reason, we then performed a thermal analysis on the same zirconia powders with the sample of Fig. 1a (Fig. 2). The DTA curve initially shows a small endothermic effect (A–B) probably due to desorption of water, and then an almost monotonic increase of heat output due to the slow combustion (B–C) of the precursor. However, at 474.3 °C a large exothermic peak (C–D) is observed. The exothermic enthalpy (~ 18.8 kJ/mol) is larger than the enthalpy (~ 5.9 kJ/mol) difference between monoclinic and tetragonal zirconia [23]. So, we can predict that this change is not due to only a phase transition. To say the least, if this exothermic peak represents a phase transition process, it should occur above 455 °C. However, the XRD

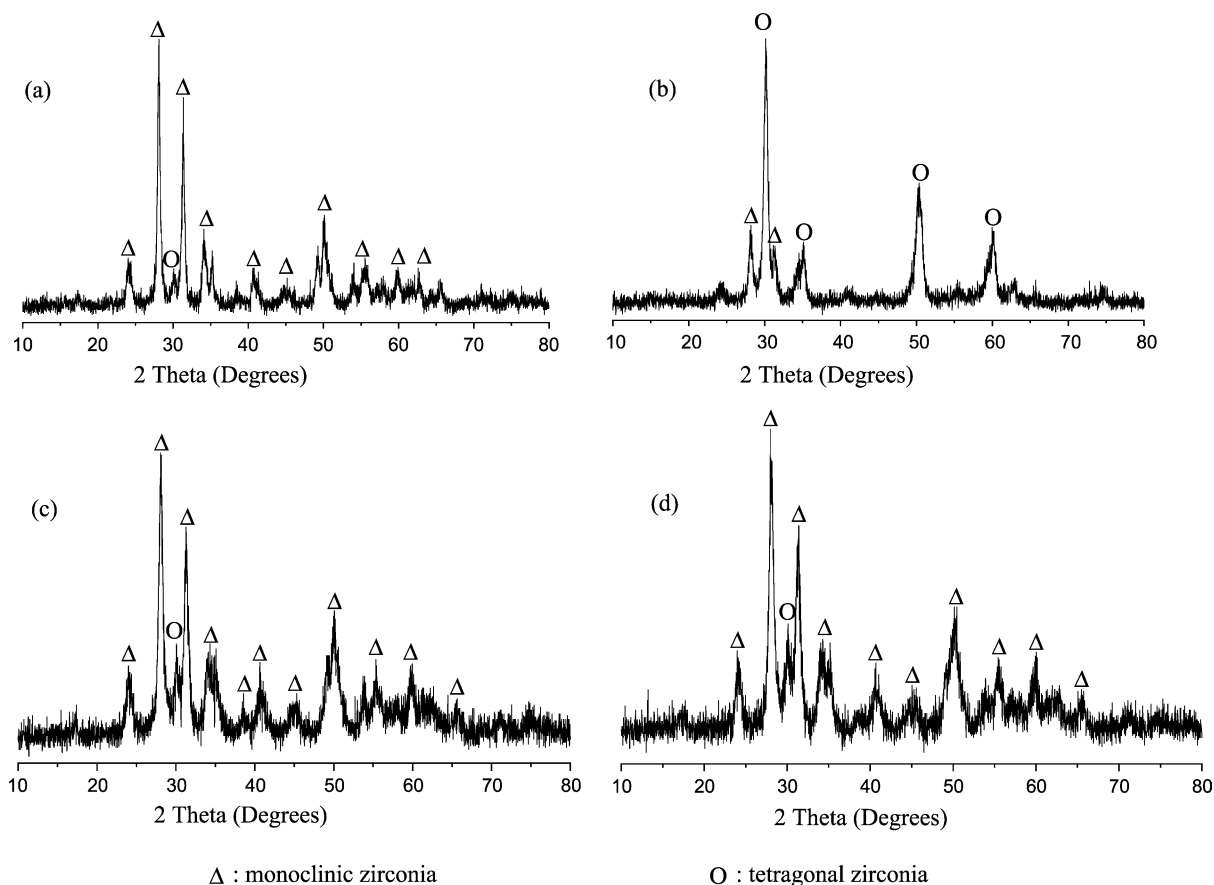


Fig. 1. X-ray diffraction patterns for zirconia powders derived from different pH precursor solutions, different reaction temperature and different calcination temperatures. (a) pH 4 and 25 °C; 600 °C, (b) pH 9.5 and 25 °C; 600 °C, (c) pH 4 and 25 °C; 450 °C, (d) pH 9.5 and 70 °C water bath; 600 °C.

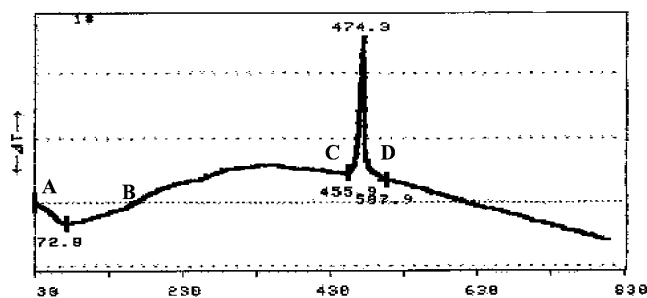


Fig. 2. DTA curve of pure zirconia xerogel for pH 4 at 20 °C/min.

analysis of the sample calcined at 450 °C (Fig. 1c) still contains 82.70% volume fraction of monoclinic zirconia, and the crystallite size (11.53 nm) is even smaller. According to the previous reports [1,20–22], the tetragonal-to-monoclinic phase transformation is impossible at this crystallite size. In a word, our experimental results indicate that the monoclinic zirconia is not transformed from the tetragonal zirconia obtained at low pHs, thus further pointing out the important role of the precursor structure. As it was interpreted in Ref. [24], the exothermic peak at 474.3 °C will be assigned to mass combustion of carbonaceous materials along with the crystallization of ZrO_2 .

In order to further investigate the effect of the reaction rate on the zirconia precursor structure, we also prepared zirconia powders in a 70 °C water bath at the same rate of alkali addition. The ZrO_2 xerogel obtained from a pH 9.5 solution was thermally treated at 600 °C, and the corresponding XRD pattern is shown in Fig. 1d. Surprisingly, the volume fraction of monoclinic zirconia reached 81.02%, much higher than the value (35.48%) determined from Fig. 1b. It is obvious that monoclinic zirconia increases at high reaction temperature, though the crystallite size (17.382 nm) does not exhibit a marked change. This result shows that the high reaction temperature could help the monoclinic phase precursor structure to form, and also shows that the polymerization rate of monomer could produce important role for the crystalline phases of zirconia.

The present experimental results indicate that both the pH and the reaction rate of precursor solution apparently affect the final structure of zirconia, which, in turn, influences the crystalline phases of the zirconia product. These results also accord well the previous experimental results [3,4,7,8,10,12]. In order to verify this by theoretical calculations, we then studied in detail the correlation between the aqueous precursor structure and the final crystalline phases structure of zirconia via selected four models based on experimental analyses and studies.

3.2. Theoretical results

Fig. 3 shows the optimized cluster structures for models named I to IV. Fig. 4 shows the ordered polymerization

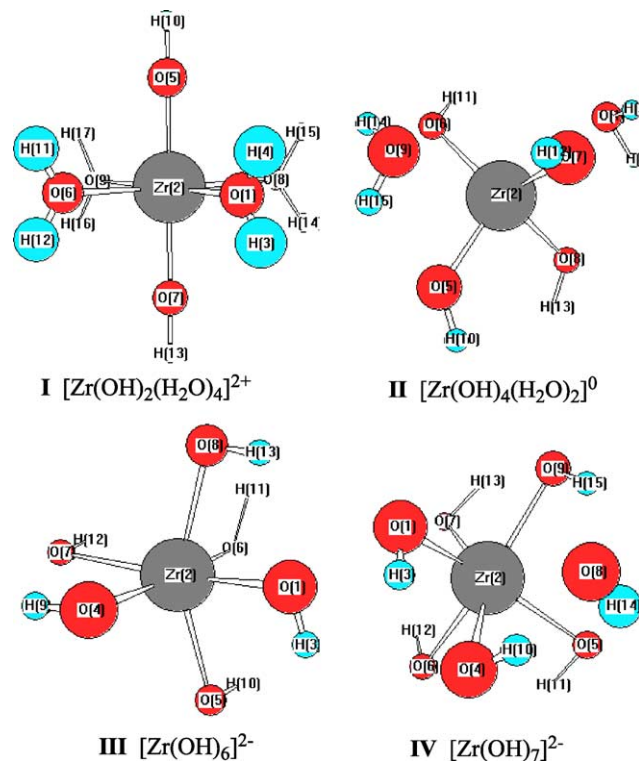


Fig. 3. Optimized cluster structures for models named I to IV.

precursor structure. Table 2 shows the interatomic distances and Mulliken charge population for the optimized cluster structures.

Model I denotes the preponderant zirconium coordination monomers in the lowest pH (<7) solutions. Because of the low hydroxyl ions concentration, water molecules are the mainly coordination body and two hydroxyl ions localize at the axial ends of the tetragonal bipyramid. A partial charge of +1.672920 a.u. was observed on zirconium atom whereas the negative charge is distributed on oxygen atoms. Charges of -0.765551 and -0.764250 a.u.

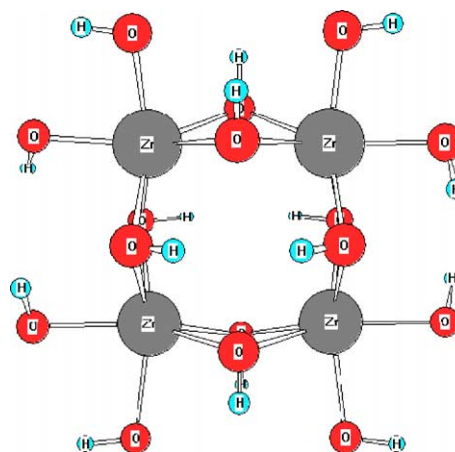


Fig. 4. The ordered structure of polymerization precursors.

Table 2

Interatomic distances and Mulliken charge populations for the optimized structure of four models used

Interatomic distance (Å)	Mulliken charge population (a.u.)
I $R(1, 2) = 2.2398$; $R(2, 5) = 1.9311$; $R(2, 6) = 2.2394$; $R(2, 7) = 1.9301$; $R(2, 8) = 2.2397$; $R(2, 9) = 2.2397$; $R(1, 3) = 0.9769$; $R(1, 4) = 0.9769$; $R(5, 10) = 0.9711$; $R(6, 11) = 0.9768$; $R(6, 12) = 0.9769$; $R(7, 13) = 0.9712$; $R(8, 14) = 0.977$; $R(8, 15) = 0.9769$; $R(9, 16) = 0.977$; $R(9, 17) = 0.9769$	$Zr_2 = 1.672920$; $O_1 = -0.804272$; $O_5 = -0.765551$; $O_6 = -0.804085$; $O_7 = -0.764250$; $O_8 = -0.804280$; $O_9 = -0.804103$; $H_3 = 0.514257$; $H_4 = 0.514244$; $H_{10} = 0.479695$; $H_{11} = 0.514196$; $H_{12} = 0.514198$; $H_{13} = 0.480016$; $H_{14} = 0.514393$; $H_{15} = 0.514172$; $H_{16} = 0.514278$; $H_{17} = 0.514170$
II $R(1, 2) = 2.4399$; $R(2, 5) = 2.024$; $R(2, 6) = 2.0205$; $R(2, 7) = 2.0208$; $R(2, 8) = 2.0241$; $R(2, 9) = 2.4412$; $R(1, 3) = 0.9773$; $R(1, 4) = 0.9767$; $R(5, 10) = 0.9667$; $R(6, 11) = 0.9683$; $R(7, 12) = 0.9683$; $R(8, 13) =$ 0.9667 ; $R(9, 14) = 0.9772$; $R(9, 15) = 0.9767$	$Zr_2 = 1.3221191$; $O_1 = -0.786074$; $O_5 = -0.824608$; $O_6 = -0.830272$; $O_7 = -0.830363$; $O_8 = -0.824525$; $O_9 = -0.7861063$; $H_3 = 0.470554$; $H_4 = 0.469041$; $H_{10} = 0.416345$; $H_{11} = 0.424013$; $H_{12} = 0.424025$; $H_{13} = 0.416344$; $H_{14} = 0.470488$; $H_{15} = 0.469018$
III $R(1, 2) = 2.1951$; $R(2, 4) = 2.1371$; $R(2, 5) = 2.149$; $R(2, 6) = 2.0977$; $R(2, 7) = 2.1326$; $R(2, 8) = 2.1274$; $R(1, 3) = 0.971$; $R(4, 9) = 0.9701$; $R(5, 10) = 0.9716$; $R(6, 11) = 0.9728$; $R(7, 12) = 0.9726$; $R(8, 13) =$ 0.9725	$Zr_2 = 0.9091041$; $O_1 = -0.889489$; $O_3 = -0.861415$; $O_5 = -0.860193$; $O_6 = -0.8449103$; $O_7 = -0.866479$; $O_8 = -0.862843$; $H_3 = 0.383405$; $H_9 = 0.377786$; $H_{10} = 0.380153$; $H_{11} = 0.375040$; $H_{12} = 0.377374$; $H_{13} = 0.382468$
IV $R(1, 2) = 2.1565$; $R(2, 4) = 2.2278$; $R(2, 5) = 2.218$; $R(2, 6) = 2.1882$; $R(2, 7) = 2.2066$; $R(2, 8) = 2.3973$; $R(2, 9) = 2.1778$; $R(1, 3) = 0.9775$; $R(4, 10) = 0.9804$; $R(5, 11) = 0.9745$; $R(6, 12) = 0.9735$; $R(7, 13) =$ 0.9721 ; $R(8, 14) = 0.9752$; $R(9, 15) = 0.9816$	$Zr_2 = 0.510373$; $O_1 = -0.859210$; $O_4 = -0.867244$; $O_5 = -0.865347$; $O_6 = -0.860163$; $O_7 = -0.886562$; $O_8 = -0.895826$; $O_9 = -0.894994$; $H_3 = 0.364385$; $H_{10} = 0.371605$; $H_{11} = 0.373557$; $H_{12} = 0.373863$; $H_{13} = 0.377215$; $H_{14} = 0.381845$; $H_{15} = 0.376501$

correspond to the hydroxyl oxygens, with values being lower than the mean charge on the oxygen atoms (-0.804185 a.u.) of coordination water. Hence, at low pH conditions, the polymerization reaction of zirconium coordination monomer mainly occurs between $Zr-H_2O$ and $Zr-H_2O$. Of course, this reaction also partially occurs between $Zr-H_2O$ and $Zr-OH$ or between $Zr-OH$ and $Zr-OH$. As listed in Table 2, the mean bond length of $Zr-OH$ is 1.93 Å, and that of $Zr-OH_2$ is 2.24 Å; it was also observed to be similar to that of bulk monoclinic zirconia [25]. Thus, these complex polymerization reactions will introduce two kinds of inequivalent bond lengths in the precursor structure, so causing an asymmetric and disordered precursor structure. The similitude between this long-distance disordered structure and that of bulk monoclinic zirconia structure probably facilitates the formation of the monoclinic phase.

Model II corresponds to preponderant zirconium coordination monomers in $pH \approx 7$ solutions. Hydroxyl ions have a larger binding energy with zirconium ion than water molecules [26], so that water molecules are gradually replaced by hydroxyl ions with the increase of pH value. The tightly coordinated hydroxyl ions localize at the four acmes of tetrahedron, and the water molecules localize at the near neighbor sites of zirconium ion. With the increase of coordination hydroxyls around the zirconium ion, the Mulliken charge of zirconium atom decreases to $+1.3221191$ a.u., whereas the mean negative charge, distributed on hydroxyl oxygen atoms increases to -0.827442 a.u., being higher than the mean charge distributed on oxygen atoms (-0.78609015 a.u.) of the coordinated water. Hence, at $pH \approx 7$ conditions, the polymerization reaction of zirconium coordination monomers mainly occurs between $Zr-OH$ and $Zr-OH$ since the polymerization reaction between $Zr-H_2O$ is not favored

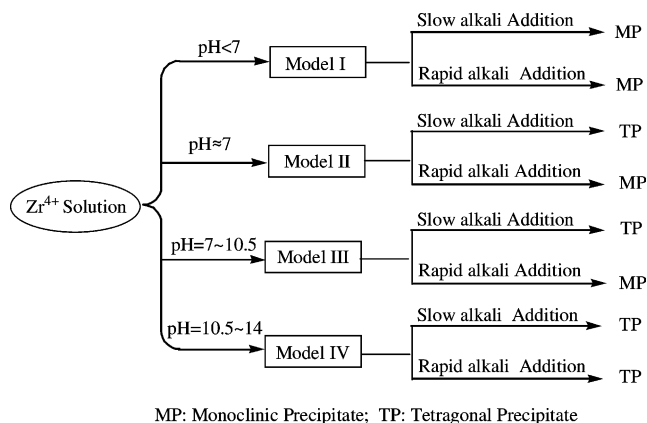
because of the relatively longer distance involved. Moreover, the flux of charge between zirconium ion and its coordination oxygens also decreases the polymerization reaction speed. For slow alkali addition, hydroxyl ions substitution is probably enough to cause the polymerization reaction mainly between $Zr-OH$ and $Zr-OH$. The almost equivalent bond lengths of $Zr-OH$ also promote the formation of a netlike ordered precursor structure, which is close to that of tetragonal zirconia. However, for rapid alkali addition, hydroxyl ions substitution may be not sufficient and will cause Models I and II describe the precursor solution. Hence, polymerization reactions will occur between $Zr-OH$ and $Zr-OH$ or $Zr-H_2O$ and $Zr-OH$. As in addition, these polymerization reactions lead to plenty of structural water in the precursor structure, so they not only introduce inequivalent bond lengths, but also disturb the netlike ordered precursor structure. Finally, this disordered precursor structure will preferentially crystallize into the monoclinic phase.

Model III identifies the preponderant zirconium coordination monomers in $pH \approx 7-10.5$ solutions. At these high pH solutions the nearest water molecules are completely replaced by hydroxyl ions, which fully occupy the six acmes of a tetragonal bipyramid. With the increase in coordination hydroxyls around the zirconium ion, the Mulliken charge of zirconium atom further decreases to $+0.9091041$ a.u., whereas the mean negative charge of hydroxyl oxygen atoms is further increased to -0.86422155 a.u. The flux of charge between zirconium ion and its coordination oxygens will help the zirconium coordination monomer to be fully replaced by hydroxyl ions, and further decreases the polymerization reaction speed between $Zr-OH$ and $Zr-OH$. This fact promotes the order of the precursor structure and further forms the precursor structure of Fig. 4. In addition, the mean bond length of $Zr-OH$, of 2.1398 Å, and

being close to the Zr–O length in bulk tetragonal zirconia [25], again promotes the formation of netlike ordered tetragonal precursor structure. Thus, for slow alkali addition, hydroxyl ions substitution is complete and polymerization reaction fully occurs between Zr–OH and Zr–OH. Once again, like Model II, hydroxyl ions substitution also may be not sufficient and easily causes Models II and III describe the precursor solution for rapid alkali addition. Hence, the netlike precursor structure will involve plenty of structural and free water, which will disturb the order in the precursor structure. The disordered precursor structure will easily crystallize into the monoclinic phase.

Model IV describes the preponderant zirconium coordination monomers in pH ~ 10.5–14 solutions. Here, not only the first neighbor water molecules but also the next neighbor ones are completely replaced by hydroxyl ions (O8 in Fig. 3). With the continuous increase of coordination hydroxyls around the zirconium ion, the Mulliken charge population of zirconium atom is further decreased to +0.510373 a.u., and the mean negative charge of hydroxyl oxygen atoms is slightly increased (–0.872253 a.u.). Hence, at the highest pH conditions, the polymerization reaction of zirconium coordination monomers again occurs between Zr–OH and Zr–OH. As in Model III, the slow polymerization reaction speed will promote the ordering of the precursor structure leading to the array shown in Fig. 4. Besides, the mean bond length of Zr–OH, now of 2.1958 Å, will also favor the formation of the netlike ordered tetragonal precursor structure. Thus, the present monomer of zirconium coordination is the most favorable for forming the tetragonal precursor structure. Moreover, the substitution of the next neighbor hydroxyl ions (O8) will prohibit the formation of Models II and III, and synchronously reduce the structural and free water of the ordered precursor structure irrespective of slow or quick alkali addition, thus leading always to the ordered cubic/tetragonal zirconia precursor structure.

The above theoretical analyses (summarized in Scheme 1) using selected models are a good explanation



Scheme 1. Outline of the theoretical results.

for the present experimental results and also accord well with the previous experimental studies [10,12]. This fact shows that our theoretical model and theoretical analyses are reasonable and believable. Thus, the present theoretical study allows building up a correlation between aqueous precursor structures and crystalline phases of zirconia. Furthermore, it would be possible to make some reasonable predictions about the precipitation, hydrolysis and condensation reactions of these complexes during the chemical processes of the precursor aqueous solution.

4. Conclusions

- (1) Nanometer zirconia powders were prepared at different pHs and different reaction temperatures using the precipitation method. X-ray results show that monoclinic zirconia is favored at pH 4 while tetragonal zirconia is favored at pH 9.5 at room temperature, and monoclinic zirconia is also favored at pH 9.5 and 70 °C reaction temperature, with the slow addition of alkali.
- (2) If Model I ($[\text{Zr}(\text{OH})_2(\text{H}_2\text{O})_4]^{2+}$ monomers) is favored in the low pH (<7) aqueous precursor solutions, it will be preferentially polymerized into monoclinic precursor structure irrespective of slow or quick alkali addition. Contrarily, if Model IV ($[\text{Zr}(\text{OH})_7]^{3-}$ monomers) is major in the high pH (>10.5) aqueous precursor solutions, tetragonal precursor structures are favored irrespective of slow or quick alkali addition.
- (3) When monomers of Model II ($[\text{Zr}(\text{OH})_4(\text{H}_2\text{O})_2]^{0}$ monomers) and Model III ($[\text{Zr}(\text{OH})_6]^{2-}$ monomers), respectively, predominate in the precursor solution, the rate of alkali addition will produce a great effect on the preferential precursor structure: tetragonal precursor structure is favored at slow alkali addition and monoclinic precursor structure is favored at rapid alkali addition.

Acknowledgements

This work was sponsored by the National Science Foundation (No. 50242008) and the Education Ministry Doctorate Foundation (No. 20020422001) of China.

References

- [1] (a) R.C. Garvie, *J. Phys. Chem.* 69 (1965) 1238. (b) R.C. Garvie, *J. Phys. Chem.* 82 (1978) 218.
- [2] F. Wu, S. Yu, *J. Mater. Sci.* 25 (1990) 970.
- [3] A. Clearfield, *J. Mater. Res.* 5 (1990) 161.
- [4] J. Livage, K. Doi, C. Mazieres, *J. Am. Ceram. Soc.* 51 (1968) 349–353.
- [5] A. Bogicevic, C. Wolverton, G.M. Crosbie, E.B. Stechel, *Phys. Rev. B* 64 (2001) 014106.

- [6] J.A. Navio, G. Colón, P.J. Sááchez-soto, M. Macias, *Chem. Mater.* 9 (1997) 1256–1261.
- [7] (a) A. Clearfield, *Inorg. Chem.* 3 (1964) 146. (b) M. Ángeles Díaz-Díez, A. Macías-García, G. Silvero, R. Gordillo, R. Caruso, *Ceram. Int.* 29 (2003) 471–475.
- [8] J. Sun, L. Gao, *J. Am. Ceram. Soc.* 85 (2002) 2382–2384.
- [9] M.C. Caracoche, P.C. Rivas, M.M. Cervera, R. Caruso, E. Benavádez, O. de Sanctis, S.R. Mintzer, *J. Mater. Res.* 18 (2003) 208–215.
- [10] R. Srinivasan, M.B. Harris, S.F. Simpson, R.J. De Angelis, B.H. Davis, *J. Mater. Res.* 3 (1988) 787–797.
- [11] R. Srinivasan, C.R. Hubbard, O.B. Cavin, B.H. Davis, *Chem. Mater.* 5 (1993) 27–31.
- [12] H.J. Noh, D.S. Seo, H. Kim, J.K. Lee, *Mater. Lett.* 57 (2003) 2425–2431.
- [13] Y. Widjaja, C.B. Musgrave, *J. Chem. Phys. B* 117 (2002) 1931–1934.
- [14] H. Toraya, M. Yoshimura, S. Somiyam, *J. Am. Ceram. Soc.* 67 (1984) 119.
- [15] B.D. Cullity, *Elements of X-Ray Diffraction*, Addison-Wesley, Reading, MA, 1978.
- [16] M.J. Frisch, G.W. Trucks, H.B. Schlegel, G.E. Scuseria, M.A. Robb, J.R. Cheeseman, V.G. Zakrzewski, J.A. Montgomery, Jr., R.E. Stratmann, J.C. Burant, S. Dapprich, J.M. Millam, A.D. Daniels, K.N. Kudin, M.C. Strain, O. Farkas, J. Tomasi, V. Barone, M. Cossi, R. Cammi, B. Mennucci, C. Pomelli, C. Adamo, S. Clifford, J. Ochterski, G.A. Petersson, P.Y. Ayala, Q. Cui, K. Morokuma, N. Rega, P. Salvador, J.J. Dannenberg, D.K. Malick, A.D. Rabuck, K. Raghavachari, J.B. Foresman, J. Cioslowski, J.V. Ortiz, A.G. Baboul, B.B. Stefanov, G. Liu, A. Liashenko, P. Piskorz, I. Komaromi, R. Gomperts, R.L. Martin, D.J. Fox, T. Keith, M.A. Al-Laham, C.Y. Peng, A. Nanayakkara, M. Challacombe, P.M. W. Gill, B. Johnson, W. Chen, M.W. Wong, J.L. Andres, C. Gonzalez, M. Head-Gordon, E.S. Replogle, J.A. Pople, Gaussian Inc., Pittsburgh PA, 1998.
- [17] A.D. Becke, *J. Chem. Phys.* 98 (1993) 1372.
- [18] P.C. Hariharan, J.A. Pople, *Theor. Chim. Acta* 28 (1973) 213.
- [19] M.S. Gordon, *Chem. Phys. Lett.* 76 (1980) 163.
- [20] J.G. Yu, M. Pan, L.M. Zhang, *China Sci. Bull.* 36 (1991) 1270 in Chinese.
- [21] G. Baldinozzi, D. Simeone, D. Gosset, M. Dutheil, *Phys. Rev. Lett.* 90 (2003) 216103.
- [22] T. Chrsaka, A.H. King, C.C. Berndt, *Mater. Sci. Engng A* 286 (2000) 169.
- [23] J.P. Coughlin, E.G. King, *J. Am. Ceram. Soc.* 72 (1950) 2262.
- [24] J.C. Ray, A.B. Panda, C.R. Saha, P. Pramanik, *J. Am. Ceram. Soc.* 86 (2003) 514–516.
- [25] D.N. Wang, Y.Q. Guo, K.M. Liang, K. Tao, *Sci. China A28* (1998) 823 in Chinese.
- [26] A.W. Thomas, H.S. Owens, *J. Am. Chem. Soc.* 57 (1935) 1825.